ELSEVIER

Hearing Research 79 (1994) 74–82

HEARING RESEARCH

Central trajectories of type II (thin) fibers of the auditory nerve in cats

Yvette V. Morgan [a], David K. Ryugo [b], M. Christian Brown [a,c,d,*]

[a] *Eaton-Peabody Laboratory, Massachusetts Eye and Ear Infirmary, 243 Charles Street, Boston, Massachusetts 02114, USA*
[b] *Center for Hearing Sciences, Johns Hopkins University, Baltimore, Maryland, USA*
[c] *Departments of Cellular and Molecular Physiology and Otology and Laryngology, Harvard Medical School, Boston, Massachusetts, USA*
[d] *Harvard-MIT Division of Health Sciences and Technology, Cambridge, Massachusetts, USA*

(Received 10 February 1994; revision received 18 May 1994; accepted 22 May 1994)

Abstract

This paper describes the central projections of thin fibers of the auditory nerve in cats. Both thin (type II) and thick (type I) fibers are labeled by extracellular injections of horseradish peroxidase (HRP) into the auditory nerve. Type I and almost all type II fibers bifurcate upon reaching the auditory nerve root of the cochlear nucleus. For a given bundle of auditory nerve fibers labeled by a discrete injection of HRP, bifurcations of type II and type I fibers are restricted to a narrow region of the nerve root. After the bifurcation, the pathways of type II branches within the anteroventral cochlear nucleus (AVCN) and posteroventral cochlear nucleus (PVCN) are similar to those of type I branches. This similarity in bifurcation and course of type I and type II fibers was observed in the ventral as well as dorsal parts of the ventral cochlear nucleus. The complete axonal course of most type II fibers could not be reconstructed, however, due to fading of the reaction product. Type II fibers produce very few collaterals in the cochlear nucleus (CN), but possess many 'en passant' swellings along their main processes and collaterals. Compared with type II fibers previously studied in mice (Berglund and Brown, 1989; 1994; Brown and Ledwith, 1990), cat type II fibers are similar in their general projections within the main body of the nucleus and in the frequency of 'en passant' swellings per length of fiber, but cat fibers have a higher percentage of 'complex' or pedunculated 'en passant' swellings.

Key words: Type II neurons; Primary afferents; Horseradish peroxidase; Cat

1. Introduction

In mammals, there are two types of primary afferent neurons connecting the hair cells of the cochlea to the cochlear nucleus (CN) of the brain. Type I fibers contact the inner hair cells of the cochlea and make up 90% to 96% of the total fibers in the auditory nerve, whereas type II fibers, which contact the outer hair cells of the cochlea, make up the remaining 4% to 10% of auditory nerve fibers (Spoendlin, 1972; Kiang et al., 1982).

The central projections of type I fibers have been well studied (Ramón y Cajal, 1909; Feldman and Harrison, 1969; Lorente de Nó, 1981; Fekete et al., 1984; Leake and Snyder, 1989; Liberman, 1991). Their projections are arranged cochleotopically in the CN, with fibers from the basal region of the cochlea projecting to the dorsal regions of the CN and fibers from the apical region of the cochlea projecting to the more ventral part of the CN. In contrast to type I fibers, less is known about the central projections of type II fibers. Both fiber types form swellings in the main body of the CN, but type II fibers additionally terminate in the surrounding granule-cell regions (Brown et al., 1988; Brown and Ledwith, 1990). Furthermore, type II fibers project cochleotopically and the regions of the CN in which the type II fiber terminates depend upon the cochlear origin of the fiber: ascending branches from fibers of the basal region of the cochlea usually terminate in the very dorsal granule-cell lamina, whereas branches from fibers originating in the apex of the cochlea terminate more ventrally, usually in the main body of the cochlear nucleus (Berglund and Brown, 1989; 1994). Regardless of cochlear origin, descending branches from type II neurons typically terminate in the granule-cell region of the CN. In general, the tonotopic mapping of type II fibers follows that of type

* Corresponding author. Fax: (617) 720-4408.

SSDI 0378-5955(94)00101-U

I fibers but differs in that type I fibers rarely if ever penetrate into the granule-cell regions.

Most of our knowledge of the central projections of type II fibers is from mice, since their small size has allowed for successful labeling of the entire type II fiber. However, there are differences between the CN of mice and cats. As classified by their appearance in Nissl-stained material, the cell types in the mouse are less distinct than they are in cats. Islands of granule cells are obvious in the cat auditory nerve root (ANR), but may be less distinct in the mouse ANR (Mugnaini et al., 1980). There may even be an additional cell type in the mouse and other rodents, the neurons of the auditory nerve nucleus, which does not appear to exist in the cat (Harrison et al., 1962; Willard and Ryugo, 1983). Most importantly, the boundaries of the granule cell region of the mouse CN are more distinct (Willard and Ryugo, 1983). These cellular differences suggest that there may also be different patterns of innervation of afferent fibers in the CN of cats. The current study investigates the central trajectories of type II fibers in the cat and compares the results to those found in the mouse.

2. Materials and methods

Eleven domestic adult cats (*Felis catus*) were used in this study. Eight of the cats were used in a previous study (Ryugo et al., 1991). Three other cats were previously used in physiological experiments in which single unit responses of the auditory nerve were recorded. Nine cats were anesthetized with i.p. injections of diallyl barbituric acid (100 mg/ml) in urethane solution (400 mg/ml) at a dose of 0.2 cc per kg body weight. Supplements of anesthetic were administered periodically in order to maintain areflexia to paw pinches. Two cats were decerebrated. The initial anesthetic for these cats prior to decerebration was an i.p. injection of sodium pentothal administered at a dose of 50 mg/kg body weight. A breathing tube was inserted into the trachea, the skin and muscle layers of the head were removed, and the skull overlying the posterior fossa was removed with rongeurs. The dura mater overlying the cerebellum was reflected, and the cerebellum was either retracted or aspirated to expose the auditory nerve and CN. Extracellular injections of horseradish peroxidase (Sigma type VI, 30% HRP in 0.1 M Tris buffer, pH 8.6) were administered using glass micropipettes (outer diameter 60–120 μm). Each injection was made iontophoretically by applying 3 μA of positive DC current (10 s on, 10 s off) for 10 min. Typically, two to three injections were made into each osseous spiral lamina, into the nerve near the Schwann-glial border, or into the most lateral portion of the cochlear nucleus.

Twenty-four to 48 h after the injections, each animal was given a lethal dose of anesthetic and perfused through the heart with isotonic saline containing 0.1% $NaNO_2$ followed by a fixative containing 1.0% paraformaldehyde and 2.5% glutaraldehyde in a 0.065 M phosphate buffer (pH 7.3) containing 0.008% $CaCl_2$. The head was removed and the brain was dissected from the skull; the CN was blocked along with a small portion of the underlying brainstem and placed in phosphate buffer in a refrigerator overnight. For seven cats, the brainstems were refrigerated in fixative overnight. The CN was then embedded in a gelatin-albumin mixture hardened with glutaraldehyde (Frank et al., 1980). Sections of 80 μm thickness were cut on a Vibratome in the modified sagittal plane, at an angle of 45° with respect to the vertical (Fekete et al., 1984), and free-floating sections were pretreated with 0.5% $CoCl_2$ in 0.1M Tris buffer, washed in phosphate buffer and reacted with 0.05% 3,3-diaminobenzidine (DAB Sigma grade II Tetra HCl, 1% DMSO and 0.01% H_2O_2) as the chromogen (Adams, 1981). The sections were mounted on 'subbed' glass slides, counterstained with thionin, and coverslipped with Permount for light-microscope analysis. Camera-lucida drawings were made and computerized planimetry was used for fiber diameter measurements.

The care and use of the animals reported on in this study were approved by the Animal Care and Use committee of the Massachusetts Eye and Ear Infirmary. The protocol title and number are 'Descending Systems to the Cochlea and Cochlear Nucleus', No. 89-02-013.

3. Results

General fiber classification

Injection sites were identified as large regions of extracellular reaction product from which labeled fibers emanated. For each animal, we could clearly identify one to three areas, the injection sites, where there were large amounts of extracellular reaction product and tissue damage. In all nerve and cochlear nucleus injections, bundles of labeled fibers extended from the injection site centrally to the cochlear nucleus and peripherally into the nerve. Each bundle contained between 85 and 265 labeled fibers. In nine nerves in which injections were made peripheral to the Schwann-glial border, we were certain that the labeled fibers were primary auditory afferent fibers. In the two CN with injections into the ANR, there were also bundles of fibers traveling centrally through the ANR as well as peripherally into the auditory nerve. Labeled fibers in these bundles are almost certainly primary auditory nerve fibers. In addition to auditory nerve fibers, however, there were other fibers labeled from

these injections in the ANR. These fibers did not travel in the bundle of labeled auditory nerve fibers, and were likely to be from other sources. Fibers not found in the auditory-nerve bundles will not be considered further in this study.

The primary afferent auditory axons within the labeled bundles were divided into two populations on the basis of fiber caliber and the presence or absence of nodes of Ranvier. Thin type II fibers averaged 0.5 ± 0.2 μm in diameter ($N = 12$), compared to an

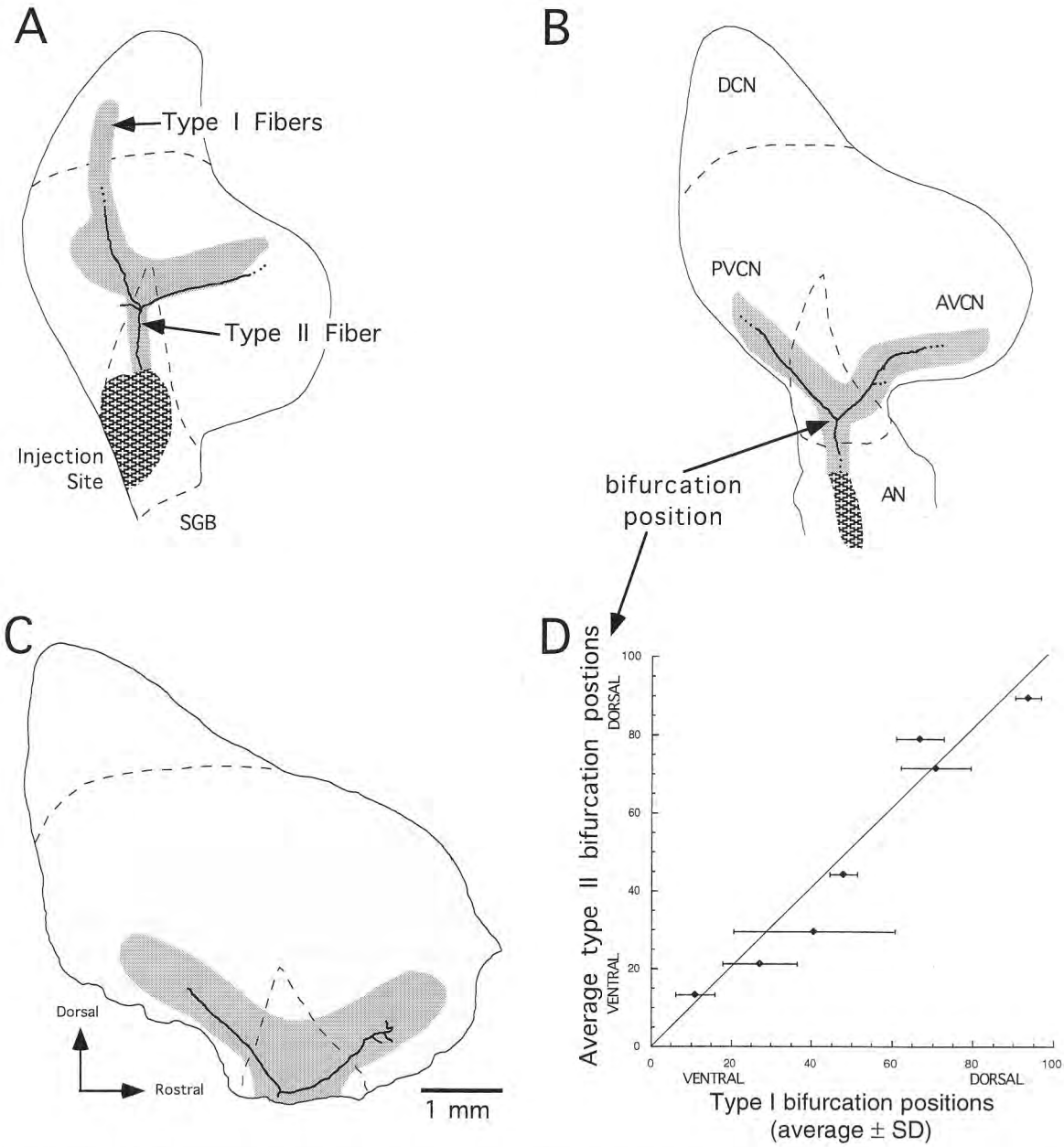

Fig. 1. (A, B, C): Camera lucida reconstructions of three type II auditory fibers labeled by injections into the auditory nerve or nerve root. (A) and (B) are partially reconstructed fibers and (C) is a completely reconstructed type II fiber. Dashed lines at the end of the fibers show where reaction product in fibers faded out. Coarse shading shows injection sites within the ANR for (A) and within the nerve for (B). In (C), the injection site, located peripheral to the cut boundary of the ANR, is not shown. Fine shading shows the boundary of labeled type I fibers within the ANR and cochlear nucleus. Dashed lines delineate boundaries of the auditory nerve root and DCN. Drawings are in the modified sagittal plane. *Please note:* (A) is originally a left cochlear nucleus; drawing was reversed to be consistent with other drawings. *Abbreviations:* AVCN: anteroventral cochlear nucleus; AN: auditory nerve; ANR: auditory nerve root; PVCN: posteroventral cochlear nucleus; DCN: dorsal cochlear nucleus; SGB: Schwann-glial border. D: The average position of type II fibers plotted against the average position of type I fibers for 7 cats in which there were 20 reconstructed type II fibers. Type I data were averages from measurements of the bifurcation positions of a group of single type I fibers labeled in the injection. One fiber that did not bifurcate is not plotted. Data are not available for the eighth injected cat.

average diameter of 2.3 ± 0.9 μm for the thick axons of type I neurons ($N = 14$). The diameter measurements for type I fibers were similar to diameters of modiolar fibers of previous studies (Liberman and Oliver, 1984; Ryugo et al., 1991). Discrete constrictions along the length of type I fibers often labeled more darkly than other regions, and were interpreted as nodes of Ranvier (Liberman and Oliver, 1984); these constrictions were absent on type II fibers.

In the three cats in which injections were placed into the osseous spiral lamina near the spiral ganglion, labeled type II axons were not observed further central to the Schwann-glial border. These injections will not be considered further.

Bifurcations and relationship to type I fibers

Type II fibers traveled centrally from the injection site and bifurcated in the ANR, forming ascending and descending branches. The ascending and descending branches usually extended from the incoming fiber to form a 'Y' shaped pattern (Fig. 1A–C). The ascending and descending branch of each fiber traveled rostrally in the anteroventral cochlear nucleus (AVCN) and caudally in the posteroventral cochlear nucleus (PVCN), respectively (Fig. 1A, B, C). Of the twenty-two fibers studied, only one fiber did not bifurcate. This non-bifurcating fiber (Fig. 2) traveled rostrally through the ANR into the posterior division of AVCN ($AVCN_p$; Brawer et al., 1974) before it could no longer be traced. Occasional, non-bifurcating, type I fibers have also been reported (Fekete et al., 1984)

Type II fibers and type I fibers that traveled in the same labeled bundle also bifurcated at the same dorso-ventral position within the ANR. For instance, the type II fiber drawn in Fig. 1A bifurcated in the dorsal part of the ANR, as did the labeled type I fibers from the same bundle (shading on Fig. 1A). Similarly, injections that labeled type II fibers that bifurcated in the ventral part of the ANR also labeled type I fibers that bifurcated in the ventral part of the ANR (Fig. 1B, C).

The bifurcation positions of type II fibers were quantified by measuring their position relative to the most ventral edge of the ANR (at the Schwann-glial border) and the dorsalmost tip of the ANR. Of the total of 22 fibers, fourteen fibers bifurcated in the ventralmost third of the ANR (0–33% from the ventral edge), four bifurcated in the middle third of the ANR

Table 1
Type II fiber lengths, collaterals, and en passant swellings (ascending branch/descending branch)

Fiber no.	Cat	Branch length (mm)	Total primary collaterals	Number of swellings/100 μm length of fiber	Number of en passant swellings			
					Ellipsoidal	Angular	Complex	Total
1 *	A	1.14/0.99	3/0	3/4	23/17	7/5	11/8	41/30
2	A	0.94/0.89	2/0	4/3	33/37	5/3	7/2	45/42
3 +	A	0.38/0.48	5/0	10/4	20/18	1/1	16/0	37/19
4	B	2.34/1.61	5/0	1/2	13/13	9/9	7/7	29/29
5 +	B	0.37/0.62	6/0	3/2	3/8	4/3	5/4	12/15
6	C	1.70/1.30	0/0	3/3	23/37	11/3	6/2	49/42
7 +	A	0.49/0.78	1/0					
8	B	1.49/1.54	2/0					
9	B	0.92/0.10	0/0					
10	B	1.50/1.10	1/0					
11	D	0.46/0.84	0/0					
12	D	0.04/1.49	0/0					
13	D	0.69/2.31	0/1					
14	D	1.86/0.88	0/0					
15	D	0.35/0.16	0/0					
16	E	0.57/1.06	2/2					
17	F	0.39/0.92	3/0					
18	B	1.62/0.93	4/0					
19 †	B	0.85/N/A	12/N/A					
20	G	0.94/1.52	1/1					
21	D	0.34/0.41	1/0					
22	H	2.56/2.08	1/3					
Total		21.9/22.0	49/7					
Average		1.00/1.05	2.3/0.3	4.1/3.2	20.7/21.7	6.2/4	8.7/3.8	35.5/29.5
Combined average		1.02		3.6	21.2	5.1	6.3	32.5
Combined percent					65.8	15.5	18.7	

* Indicates the completely reconstructed type II fiber; + Indicates the reconstructed ascending branches with one fading collateral. The swelling counts encompass swellings along the branches and their collaterals. † This fiber did not bifurcate, therefore, the branch length and number of collaterals are counted along the entire length of the fiber.

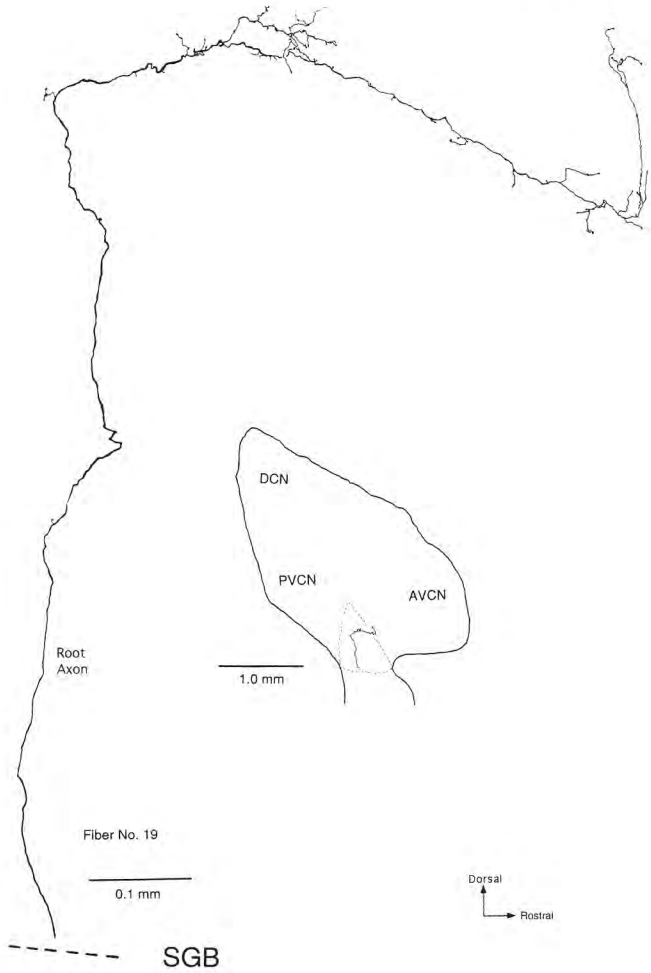

Fig. 2. Camera lucida tracing of the branching pattern of one type II fiber. This fiber did not bifurcate and terminated in an typical caudal AVCN. Inset shows the position of the type II fiber within the cochlear nucleus. SGB: Schwann-glial border.

(33–67% from the ventral edge), and three fibers bifurcated in the dorsalmost third (68–100% from the ventral edge). The topographical arrangement of type II bifurcations was similar to the arrangement of type I bifurcations (Fig. 1D). For instance, for any bundle of labeled fibers, the type II fibers bifurcated within the range of the type I bifurcations. This pattern was true for ventral, medial, and dorsal bifurcating bundles. There was no tendency for type II fibers to bifurcate dorsally within the type I bifurcations as was previously observed in mouse (Brown and Ledwith, 1990).

The ascending and descending branches of both types of fibers traveled together for long distances in the AVCN and PVCN (Fig. 1A, B, C). The type II fibers became progressively lighter as they coursed from the injection site centrally into the VCN. Eventually, the reaction product in most fibers faded completely. Increasing the survival time from 24 to 48 h did not increase the labeling in more central regions (present results; Ryugo et al., 1991). The length of the ascending branches from bifurcation point to fading averaged 1.0 ± 0.7 mm ($N = 22$; Table 1). The length of the descending branch from bifurcation to fading averaged 1.0 ± 0.6 mm ($N = 22$). The longest ascending branch was 2.6 mm in length (fiber 22) and the longest descending branch was 2.3 mm in length (fiber 13). The average length of the type II fibers from injection site to bifurcation was 1.1 mm ($N = 13$) and the longest length from injection site to the bifurcation was 1.7 mm.

Branching pattern

In general, type II fibers were sparsely branched, but their main axons did form a few collaterals in the nerve root ('root collaterals'), while their ascending and descending branches formed collaterals in more medial locations. Root collaterals, like other collaterals, were thinner than the main type II fiber. These collaterals were usually emitted perpendicular to the main axon and traveled only for short distances before ending in a terminal swelling (or fading); all root collaterals measured less than 85 μm in length. We counted the number of root collaterals on individual type II fibers, only including fibers that had a course in the nerve root that was not obscured by an injection site. Four of these eleven fibers (36%) gave off collaterals along their root axon. Three of the four fibers possessed only one root collateral, while the fourth fiber possessed three root collaterals. Two of the fibers that formed root collaterals were ventral fibers while the other two were middle fibers.

Type II fibers also rarely gave off primary collaterals along the length of their main branches (Fig. 1A, B, C). We totaled the number of collaterals on the ascending and descending branches of all of the fibers and divided that number by the total length of both branches for all fibers. All measurements were made central to the bifurcation point. For the ascending branches of all 22 fibers, there were 49 collaterals and a total summed branch length of 21.9 mm, which is an average of one collateral every 0.5 mm length of branch (Table 1). The descending branches possessed fewer collaterals: 7 collaterals and a total branch length of 22.0 mm, yielding an average of only one collateral every 3.1 mm length of branch. Overall, when ascending branches and descending branches are combined, type II fibers averaged one collateral for every 0.8 mm length of branch, or 1.3 collaterals per millimeter of branch. However, there was some variation in the branching patterns displayed by individual fibers. Most of the fibers had a few collaterals along the main branches. Two of the fibers (Figs. 2 and 3), however, displayed many small collaterals within short intervals along the ascending branches. Both of these fibers were labeled from auditory nerve injections.

Collaterals of the ascending and descending branches usually faded before their endings could be traced, but were reconstructed up to 1026 μm in length. The average collateral was 79 ± 138 μm in length before fading ($N = 56$). Most of the collaterals were unbranched. However, two collaterals exhibited an elaborate network of smaller branches and terminal swellings. The most profusely branched network is illustrated in Fig. 3. These collateral arborizations occurred near the bifurcations of a middle and ventral fiber. In one case, these collaterals terminated near a granule cell 'island' within the ANR (Fig. 3). However, the second network did not terminate near a granule cell 'island'.

Although the reaction product in most of the type II fibers faded out, one of the type II fibers was 'completely' reconstructed because all branches could be traced to terminal swellings in the middle of sections. This fiber (Fig. 1C) bifurcated at a point 16% of the distance from the ventral edge of the ANR. The ascending branch traveled for 1.1 mm into the anterior division of the AVCN ($AVCN_a$) and ended in a terminal swelling (Table 1, fiber 1), after giving off three collaterals that also ended in terminal swellings. The collaterals measured 40 μm, 101 μm, and 109 μm in length. The descending branch traveled for 1.0 mm into the PVCN and also formed a terminal swelling. The descending branch remained unbranched throughout its course. Though the reaction product within this fiber became lighter as it traveled away from the injection site, we are confident that both branches were traced completely.

Of the fibers that were partially reconstructed, three fibers had ascending branches that appeared complete except for one collateral (Table 1, fibers 3, 5, and 7). The collaterals that faded were located along the centralmost quarter of the ascending branches, but the tips of the ascending branches were reconstructed to terminal swellings in $AVCN_p$. The descending branches of these fibers faded in PVCN before the terminal swellings were reached.

Swellings from type II fibers

There are two general classifications of swellings on type II fibers: terminal swellings and 'en passant' swellings. Few terminal swellings were observed at the ends of the ascending and descending branches or at the tips of collaterals. This circumstance was most likely due to the low number of collaterals given off by type II fibers as well as the tendency of our fibers to

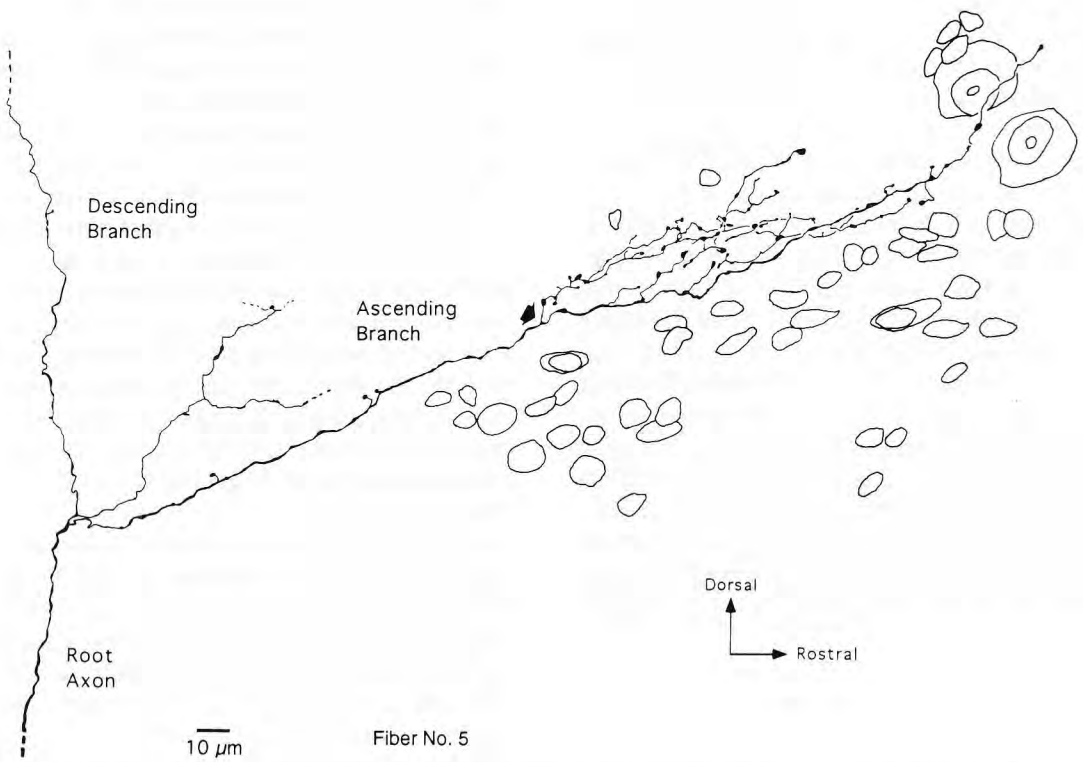

Fig. 3. Camera lucida tracing of the elaborate branching pattern of one type II collateral in the auditory nerve root (ANR). Arrow points to the branch point of a collateral that formed many branches and swellings. The root axon enters the figure from the lower left of the illustration. The descending branch exits the illustration at the upper left; it was traced 0.62 mm farther into the dorsalmost nerve root. Cells drawn without nuclei represent granule cells; those with nuclei indicate larger cells.

fade as they traveled centrally from the injection site. The completely reconstructed fiber had only five terminal swellings, four on the ascending branch and its collaterals, and one on the descending branch. In general, terminal swellings appeared spherical with a smooth surface when viewed under a light microscope.

Type II fibers and collaterals had numerous varicosities or *en passant* swellings. We counted the number of 'en passant' swellings (Table 1) on six cat type II fibers, chosen because they were the most completely reconstructed. This data set contained the one completely reconstructed type II fiber, two fibers that had mostly reconstructed ascending branches and partially reconstructed descending branches, and three fibers that could not be fully reconstructed. For this data set, the ascending branches and their collaterals averaged 1144 μm in length and the descending branches averaged 982 μm from the points of bifurcation to the points at which they could no longer be traced in $AVCN_p$ and rostral PVCN, respectively. An 'en passant' swelling was counted if it exceeded twice the diameter of the fiber from which it emanated. The number of swellings per 100 micron length of fiber ranged from 1 to 10 (Table 1). There was little difference in the number of 'en passant' swellings between ascending and descending branches of type II fibers (4 swellings per 100 μm length of fiber on the ascending branch versus 3 swellings per 100 μm length of fiber on the descending branch).

En passant swellings were classified as ellipsoidal, angular, or complex in shape depending upon their appearance under a light microscope. Ellipsoidal swellings appeared ellipsoidal when viewed from all planes of focus. Swellings that had an angular appearance but no other distinguishing characteristics were classified as angular. Complex swellings were characterized as possessing one or more short (< 5 μm) protuberances emitting from one side of the swelling (Brown and Ledwith, 1990). Most of these protuberances were short stalks capped with a swelling; they have also been termed pedunculated swellings (Ryugo et al., 1991). There were no great differences in the percentages of ellipsoidal, angular, and complex swellings between ascending and descending branches. When the ascending and descending branches were combined, our counts indicate that 65.8% of the swellings were ellipsoidal, 15.5% of the swellings were angular, and 18.7% of the swellings were complex (Table 1).

4. Discussion

Type II trajectories

In this paper we have labeled type II auditory nerve fibers and traced them into the CN of the cat. Although much of the central axons were reconstructed, most fibers could not be traced all the way to their terminals due to fading of the reaction product. Similar to type I fibers, type II fibers traveled into the CN and bifurcated, forming ascending and descending branches. The topographical relationship between type I and type II fibers was well-maintained as far as the bifurcation position and the initial course through the main body CN. Peripherally, type I and type II fibers from the same types of discrete injections that we have made generally project from the same spiral ganglion region to the same region within the organ of Corti (Simmons and Liberman, 1988). In the organ of Corti, type II fibers (outer spiral fibers) spiral basally as much as a quarter octave to contact outer hair cells whereas type I fibers (radial fibers) do not spiral but immediately contact inner hair cells directly (Brown, 1987; Simmons and Liberman, 1988). Our results mean that except at the hair cells, type I and type II fibers from the same region of the spiral ganglion have similar courses in the auditory nerve, the ANR, and the main body of the CN. These results are very similar to those from studies of type II fibers in the mouse, gerbil, and guinea pig (Brown, 1987; Brown and Ledwith, 1990; Berglund and Brown, 1994).

The fully reconstructed and mostly reconstructed ascending branches of four type II fibers traveled far into $AVCN_p$ of the cat and terminated. All of these fibers bifurcated ventrally and the ascending branches showed a pattern of innervation that is similar to ventral fibers from the mouse (Berglund and Brown, 1994). In mouse, however, a few ventrally-bifurcating type II fibers traveled beyond to the rostral edge of the magnocellular region to the superficial layer of granule cells. Due to fading, however, we could not determine if this pattern was also shown by cat fibers. Furthermore, there were differences in the form of the descending branch. For the single descending branch that was completely reconstructed in the cat, the site of termination was in the PVCN. This innervation pattern is different from the pattern seen in the mouse. In mouse, descending branches from all type II fibers travel through the PVCN to the granule cell lamina that divides PVCN from DCN (Berglund and Brown, 1994).

At present, however, one can only guess at the appearance of the ultimate terminations of type II fibers in cats. Cat type II fibers were labeled approximately the same distance as rodent fibers, but a proportionally smaller length of their entire course was labeled. For gerbil type II fibers that were completely reconstructed, the distance from the injection site to the AVCN endings was typically 3.3 mm and the distance from the injection site to the endings in the DCN was typically 4.7 mm (Brown et al. 1988). However, many gerbil fibers faded before their terminals were

reached so average lengths of all fibers would be much shorter. The longest cat type II fiber (fiber 22) was at least 4.3 and 3.8 mm in length from the general vicinity of the injection site to fading of the ascending and descending branches, respectively, and the average lengths of cat type II fibers were 2.1 mm from injection site to fading. Therefore, there my be little difference in average transport distance between cat and gerbil in spite of species differences and differences in injection site.

Type II branching patterns

At first glance, cat type II fibers formed fewer collaterals in the cochlear nucleus than mouse type II fibers, since on average, cat fibers exhibited 1.3 collaterals per millimeter of branch compared to 11.1 collaterals per millimeter of branch for mice (Brown and Ledwith, 1990). This difference, however, may be artificially due to the differences in the portion of the fibers that was used for counting, because many of the mouse collaterals are formed near the tips of the ascending and descending branches, rather than near the bifurcations. By contrast, the current sample from cats mostly includes fibers near their bifurcations, but lacks fibers near their tips. To quantify the cat-mouse differences, we performed a scaled analysis on mouse type II fibers by counting the number of collaterals on the half of the ascending and descending branches closest to the bifurcation. In this scaled analysis, the mouse ascending and descending branches both averaged 2.9 collaterals per millimeter length of branch, closer to the 1.3 collaterals per millimeter found on the cat fibers. At most, the scaled mouse fibers possessed two collaterals on their ascending and descending branches. If cat fibers have a similar branching pattern as mouse fibers, they should have more collaterals near their tips. However, because the cat type II fibers faded before their endings could be reached, the exact branching pattern of cat type II fibers must remain an open question.

There were, however, some differences in fiber branching patterns that merit further discussion. The collaterals along cat type II fibers showed an additional branching pattern to that seen in mouse type II collaterals. In mouse, the branching patterns remained very simple; the collaterals were unbranched or had one or two smaller branches off the main fiber (Brown and Ledwith, 1990). In cats, we noticed both the simple pattern and the complex network of branches and swellings (Fig. 3). This complex network of collaterals and swellings was never observed in the mouse. Perhaps this difference is due to the fact that islands of granule cells are less prevalent in the mouse ANR (Mugnaini et al., 1980). It has been hypothesized that type II fibers terminate on granule cells (Brown et al., 1988). The complex network of cat type II collaterals is reminiscent of arborizations displayed along unmyelinated, thin fibers in other systems, such as the C-fibers of the somatosensory system (Sugiura et al., 1986).

Type II swellings

We found similarities and differences between cat and mouse type II fibers for 'en passant' swellings. The frequency of *en passant* swellings along the length of cat and mouse type II fibers was very similar. In cat, type II fibers had an average of 3 to 4 swellings per 100 μm length of fiber. Mouse type II fibers averaged 5 swellings per every 100 μm of fiber (Brown and Ledwith, 1990). In cat and mouse, there was little difference in the number of swellings per 100 μm of fiber between ascending and descending branches. Type II fibers in the cat, however, had more pedunculated or complex swellings than mouse type II fibers. We found that 19% of the 'en passant' swellings on cat type II fibers were complex swellings; this type of swellings composed only 7% of the swellings on mouse type II fibers (Brown and Ledwith, 1990). Due to the small number of terminal swellings observed on cat type II fibers, 'en passant' swellings may represent the numerically most important areas for synapse formation. Although many type II 'en passant' swellings have been shown to lack features typically associated with synapses, pedunculated swellings have been shown to form synapses (Ryugo et al., 1991; Berglund et al., 1991). Thus pedunculated swellings are likely to be significant in terms of information transferred to the central nervous system.

Acknowledgments

Sincere thanks are due to A.M. Berglund, L.W. Dodds, T.S. Liu, and D.D. Simmons for technical assistance with this project. We also thank A.M. Berglund for her helpful comments to the manuscript. This work was supported by NIH grants DC 01089, DC 00119, and DC 00232.

References

Adams, J.C. (1981) Heavy metal intensification of DAB-based HRP reaction product. J. Histochem. Cytochem. 29, 775.

Berglund, A.M. and Brown, M.C. (1994) Central trajectories of type-II spiral ganglion cells from various cochlear regions in mice. Hear. Res. 75, 121–130.

Berglund, A.M., Benson, T.E. and Brown, M.C. (1991) Synapses from type II primary afferent fibers in the mouse cochlear nucleus. 14th Assoc. Res. Otolaryngol. February 1991.

Brawer, J.R., Morest, D.K. and Kane, E.C. (1974) The neuronal architecture of the cochlear nucleus of the cat. J. Comp. Neurol. 155, 251–300.

Brown, M.C. (1987) Morphology of labeled afferent fibers in the guinea pig cochlea. J. Comp. Neurol. 260, 591–604.

Brown, M.C., Berglund, A.M., Kiang, N.Y.S. and Ryugo, D.K. (1988) Central trajectories of type II spiral ganglion neurons. J. Comp. Neurol. 278, 581–590.

Brown, M.C. and Ledwith, J.V., III. (1990) Projections of thin (type-II) and thick type-I auditory-nerve fibers in the cochlear nucleus of the mouse. Hear. Res. 49, 105–118.

Fekete, D.M., Rouiller, E.M., Liberman, M.C. and Ryugo, D.K. (1984) The central projections of intracellularly labeled auditory nerve fibers in cats. J. Comp. Neurol. 229, 432–450.

Feldman, M.L. and Harrison, J.M. (1969) The projection of the acoustic nerve to the ventral cochlear nucleus of the rat. A Golgi study. J. Comp. Neurol. 137, 267–294.

Frank, E., Harris, W.A. and Kennedy, M.B. (1980) Lysophosphatidyl choline facilitates labeling of CNS projections with horseradish peroxidase. J. Neurosci. Methods 2, 183–189.

Harrison, J.M., War, W.B. and Irving, R.E. (1962) Second order neurons in the acoustic nerve. Science 138, 893–895.

Kiang, N.Y.S., Rho, J.M., Northrop, C.C., Liberman, M.C. and Ryugo D.K. (1982) Hair-cell innervation by spiral ganglion cells in adult cats. Science 217, 175–177.

Leake, P.A. and Snyder, R.L. (1989) Topographic organization of the central projections of the spiral ganglion in cats. J. Comp. Neurol. 281, 612–629.

Liberman, M.C. (1991) Central projection of auditory-nerve fibers of differing spontaneous rate. I. anteroventral cochlear nucleus. J. Comp. Neurol. 313, 240–258.

Liberman, M.C. and Oliver, M.E. (1984) Morphometry of intracellularly labeled neurons of the auditory nerve: Correlations with functional properties. J. Comp. Neurol. 223, 163–176.

Lorente de Nó, R. (1981) The Primary Acoustic Nuclei. Raven Press, New York.

Mugnaini, E., Warr, W.B. and Osen, K.K. (1980) Distribution and light microscopic features of granule cells in the cochlear nucleus of cat, rat, and mouse. J. Comp. Neurol. 191, 581–606.

Ramón y Cajal, S. (1909) Histologie du Système Nerveux de l'Homme et des Vertébrés. Vol. I. Madrid: Instituto Ramón y Cajal (1952 reprint), pp. 754–838.

Ryugo, D.K., Dodds, L.W., Benson, T.E. and Kiang, N.Y.S. (1991) Unmyelinated axons of the auditory nerve in cats. J. Comp. Neurol. 308, 209–223.

Simmons, D.D. and Liberman, M.C. (1988) Afferent innervation of outer hair cells in adult cats: I. Light microscopic analysis of fibers labeled with horseradish peroxidase. J. Comp. Neurol. 270, 132–144.

Spoendlin, H. (1972) Innervation densities of the cochlea. Acta Otolaryngol. 73, 235–248.

Sugiura, Y., Lee, C.L. and Perl, E.R. (1986) Central projections of identified, unmyelinated (C) afferent fibers innervating mammalian skin. Science 234, 358–361.

Willard, F.H. and Ryugo, D.K. (1983) Anatomy of the central auditory system. In: J.F. Willott (Ed.), The Auditory Psychobiology of the Mouse, Charles C Thomas, Springfield, IL, pp. 201–304.